FINITE DIFFERENCE SIMULATION OF LOW CARBON STEEL MANUAL ARC WELDING

by

Moneer H. AL-SA'ADY [a], ***Mudar A. ABDULSATTAR*** [b*], ***and Laith S. AL-KHAFAGY*** [a]

[a] Foundation of Technical Education,Technical College-Baghdad, Baghdad, Iraq
[b] Directorate of Materials Science, Ministry of Science and Technology, Baghdad, Iraq

Original scientific paper
UDC: 621.791.053:66.011:669.15-194
DOI: 10.2298TSCI100206055S

This study discusses the evaluation and simulation of angular distortion in welding joints, and the ways of controlling and treating them, while welding plates of (low carbon steel) type A-283-Gr-C through using shielded metal arc welding. The value of this distortion is measured experimentally and the results are compared with the suggested finite difference method computer program. Time dependent temperature distributions are obtained using finite difference method. This distribution is used to obtain the shrinkage that causes the distortions accompanied with structural forces that act to modify these distortions. Results are compared with simple empirical models and experimental results. Different thickness of plates and welding parameters is manifested to illustrate its effect on angular distortions. Results revealed the more accurate results of finite difference method that match experimental results in comparison with empirical formulas. Welding parameters include number of passes, current, electrode type and geometry of the welding process.

Key words: *finite difference method, welding, low carbon steel*

Introduction

Welding processes depends on local heating of the welded parts up to melting temperature. Simulations of welding relays on the solution of heat transfer equations accompanied with the appropriate mechanical equations. These solutions started at the thirties of the twentieth century as analytical solutions [1]. After 30 years more accurate numerical solutions started to appear [2]. The evolution of these solutions was a direct result of the advances in computer speeds. Numerical methods include mostly two methods, finite element method (FEM) and finite difference method (FDM) and their derivatives. Other less known methods also exists [3]. Finite difference method is more than a mid way between solutions of the over complicated FEM and simple analytical solutions. It is always possible to reduce the size of the uniform mesh steps encountered in FDM to account approximately for curved geometrical parts [4]. FDM main variables are temperature, time, geometry, and materials properties. This method is still evolving to reduce large computer times of the 3-D case [4].

* Corresponding author; e-mail: mudarahmed3@yahoo.com

Many kinds of distortions of the welded pieces occur during the welding process such as longitudinal, transverse, buckling, and angular distortions. These distortions are due to the heating and cooling of both welded and filler materials. In this work we shall concentrate on angular distortions. Simplified empirical equations were suggested previously to calculate angular distortions such as [5, 6] which we will compare with our results. Numerical simulations of welding are not confined to arc welding but can be also found in other methods such as laser welding [7-10]. Sophisticated numerical programs and methods are now in a position that can yield accurate and reliable results [11-15]. In spite of being one of the first suggested numerical methods, finite difference method is still used in many branches of thermal and mechanical calculations [16-22] because of its speed and simplicity especially in simple geometrical cases.

Theory

In this work transient heat conduction equation is solved using FDM. This equation in Cartesian co-ordinates is given by:

$$\frac{\partial T}{\partial t} = \frac{\lambda}{\rho c}\left(\frac{\partial^2 T}{\partial x^2} + \frac{\partial^2 T}{\partial y^2} + \frac{\partial^2 T}{\partial z^2}\right) + \frac{Q}{\rho c} \tag{1}$$

In this equation, T, t, λ, ρ, and c are the temperature, time, thermal conductivity, density, and heat capacity, respectively. Q is the volumetric density of the power input. This factor also includes the volumetric power due to phase transformation such as melting, solidification, or reaction. The sum of Q over all the meshes that receives electrical power of the electrode is equal to the electrical power (IU) times the efficiency. At the boundary, heat is exchanged with the outer environment via convection or radiation. Heat convection is described by the following equation:

$$q_c = hA(T_w - T_\infty) \tag{2}$$

where T_w is the surface temperature, T_∞ – the temperature of the surrounding fluid, A – the surface area, and h – the convection heat transfer coefficient. Heat radiation is described by the equation:

$$q_r = F_\varepsilon F_G \sigma A(T_w^4 - T_\infty^4) \tag{3}$$

where F_ε and F_G are emmissivity and geometry coefficients, respectively. σ is the Stefan--Boltzman constant. FDM with equal meshing in 3-D (FORTRAN language program) is used to simulate the welding processes. Input to the simulation program includes thermal conductivities, densities, heat capacities emmissivity coefficient, convection coefficient, and geometry of the welded pieces and their surroundings. Current, voltage, efficiency of the welding machine are also given as an input to the simulating program. The FDM is used to solve heat transfer equations including conduction, convection, and radiation. The simulation process includes two steps. The first step is concerned with the simulation of electrode heating and melting. Not all the input welding power is converted to heating the electrodes. Some of this power is lost in other parts of the electrical circuit. The overall efficiency is approximately 50% in most welding processes. This step shows that radiation is the dominant heat loss process due to the high temperature of the molten electrode and high emmisivity of steel. Convection through air and conduction of heat are less important in this step. The second step investigates the cooling of the molten electrodes in the joints and its effects on the

welded plates. 3-D temperature distribution in the welded pieces are given as an output of the program and used to understand the extent at which the material of welded pieces are affected by the heat input of the welding processes. The angular distortions are also given as an output depending on the welding process parameters. These angular distortions are caused by thermal stresses, plastic deformation, and phase transformation (liquid to solid transformation) [23, 24]. Cooling rates and temperatures of the various parts is shown to interpret the microstructure and properties of the weld and base plates. These rates can be optimized and correlated to welding quality. Simplified empirical equations were suggested previously to calculate angular distortions such as [5]:

$$\beta = 2\alpha T_{\mathrm{S}} \tan\frac{\theta}{2} \tag{4}$$

where α is the thermal expansion coefficient, T_{S} – the softening material temperature which is 600 °C for steel, and θ is the groove angle. Another equation is given by [6]:

$$\beta = 0.13\frac{IU}{vH^2} \tag{5}$$

where I is the current, U – the applied voltage, v – the welding speed, and H – the plate thickness. The above empirical equations and other related equations give rise to different errors depending on their sophistication and range of applicability.

Experimental procedure

Two plates of 200 × 100 mm sides are used. The welding is on the 100 mm side. Different thickness of plates is also used to explore the effect of welded pieces thickness on temperature distribution and angular distortions. This included 4, 6, and 10 mm plates. A welding speed of 78 mm/min. is chosen. The current and voltage with the values of 24 V and 100 to 150 A is used with E 6010 and E 7018 electrodes. The electrodes diameter is 2.5 and 3.23 mm. Square and single butt joints are investigated (shape of plates prepared space for welding). One, two and three passes is used to fill the joints. The above dimensions and materials cover ranges that is around the consistent ASME (American Society for Mechanical Engineers) standards and ends slightly above the ASME standards. A welding machine (ESAB) is used. The plates are prepared by the above mentioned dimensions, cleaned and grooved in square or single-v butt joints. Materials properties that include thermal and mechanical properties can be found in references such as [23].

Results and discusion

Generally, the value of angular distortions increases with the increase of input current. The kind, geometry, and shape of the joints also affect the values of angular distortions. Mesh size of 1 mm is used in discretizing FDM in 3-D space. The shapes and geometries described in the experimental procedure section are used in the simulating program. In addition to the above-mentioned geometries, the two welded pieces are 2 mm apart (at the root part of the welded pieces) at the beginning of the welding processes. In fig. 1 an upper view of the two welded pieces shows that temperature decreases quickly when the welding process proceeds. Since the electrode melts down and fills some of space (depending

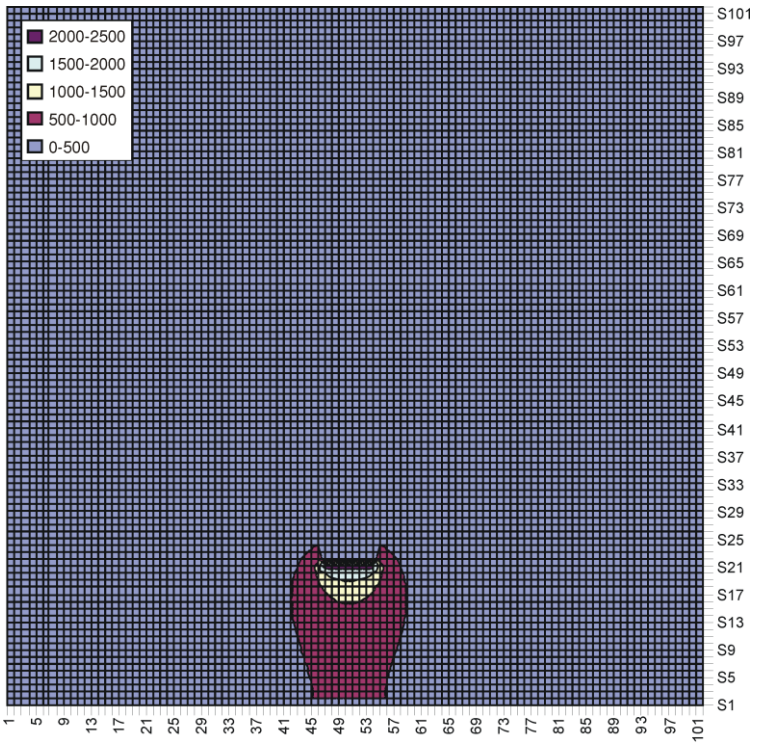

Figure 1. Upper view shows the distribution of temperatures (in ˚C) between the two welded pieces after 15 seconds as welding process proceeds; numbers on the axes represent mesh numbers of FDM (color image see on our web site)

on welding speed) between welded pieces as a liquid, the temperature profile shape would be like a line at the highest gradient temperature region. The value of temperature is less than half the original welding temperature just 5 mm after the advance of welding electrode. Figure 2 also shows the same reduction of temperature but in time scale. In this figure temperature re-

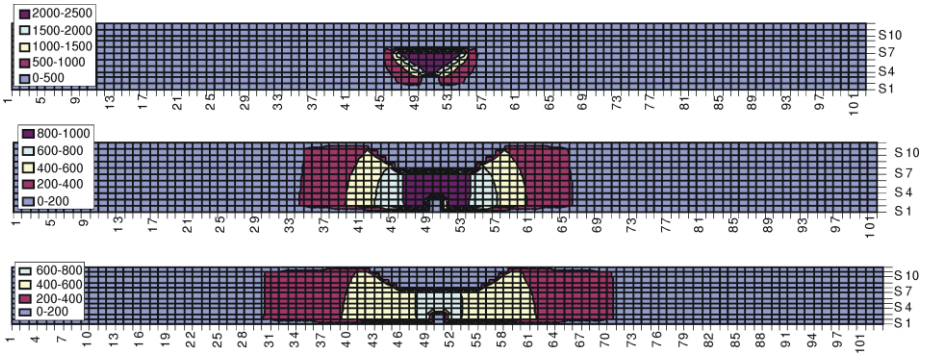

Figure 2. Sectional view of temperature distribution (in ˚C) of the two welded pieces at 1, 7, and 13 seconds from the starting of welding process; numbers on the axes represent mesh numbers of FDM (color image see on our web site)

duces to less than half the original welding temperature in just 7 seconds. Because of rapid solidification, the electrode melt will not have time to fill the space between the two electrodes at the weld root. This space will still have the ambient air temperature which is categorized from 0 to 200 °C. These two figures show the sharp temperature disintegration in both space and time co-ordinates. Figure 2 (7, 13 s) shows that temperature disintegration slows down as temperatures reduces to less than 1000 °C. Table 1 shows experimental and theoretical angular distortions in welding 6 mm thickness plates in one pass using single-v butt joints. In this table we can see that increasing the current does not always increases the angular distortion. This is due to the fact that increasing the current results in some fluid flow of the molten filler and base metal material which is not taken into account in the present FDM. However, the results of FDM are far better than the general empirical equations. Using more than one welding pass complicates the situation further. It is obvious from the results of tab. 2 that increasing the number of passes decreases the value of angular distortion but this has an economical loss of additional filler material and efforts. Tables 3 and 4 compares the effect of using two and three passes on the angular distortions. Three passes shows less angular distortions than two passes. However an optimal current must be chosen to obtain the minimum distortions. In the last table (tab. 5) a square butt joint is used. The angular distortions in this case are less than the comparable single-v joints. This is due to the fact that a contraction of the solidified filler molten material is equal both on the surface and inner part of the joint. However, square joints need more filler or electrode material than single v-joints. This also confirms that geometry has an important effect on angular distortion.

Table 1. Experimental and theoretical angular distortions in welding 6 mm thickness plates in one pass using single-v butt joints

Welding speed [mms^{-1}]	Voltage [V]	Current [A]	Electrode diameter [mm]	Electrode type	Empirical eq. 4 (10^{-2} radians)	Empirical eq. 5 (10^{-2} radians)	Finite diference computed angular distortion (10^{-2} radians	Practical angular distortion (10^{-2} radians)
78	22	80	2.4	E7018	1.44	8.14	5.865	4.971
78	22	100	2.4	E7018	1.44	10.18	6.248	6.995
78	22	125	2.4	E7018	1.44	12.73	6.648	5.369

Table 2. Angular distortions in welding 6 mm thickness plates in two opposite pass using single-v joints; angular distortions are in radians

Amperage of 1st run of welding (2.4 mm diameter of welding electrode)	Amperage of 2nd run of welding (3.25 mm diameter of welding electrode)	Angular distortion (10^{-2} radians)
80 A	100 A	2.011
100 A	125 A	2.145
125 A	150 A	1.752

Table 3. Angular distortions in welding 10 mm thickness plates in two opposite pass using single-v joints

Amperage of 1st run of welding (2.4 mm diameter of welding electrode)	Amperage of 2nd run of welding (3.25 mm diameter of welding electrode)	Angular distortion (10^{-2} radians)
80 A	100 A	4.482
100 A	125 A	4.612
125 A	150 A	3.719

Table 4. Angular distortions in welding 10 mm thickness plates in three opposite pass using single-v joints

Amperage of 1st run of welding (2.4 mm diameter of welding electrode)	Amperage of 2nd and 3rd run of welding (3.25 mm diameter of welding electrode)	Angular distortion (10^{-2} radians)
80 A	100 A	3.422
100 A	125 A	1.611
125 A	150 A	2.032

Table 5. Angular distortions in welding 4 mm thickness plates in three opposite pass using square butt joints

Amperage of 1st run of welding (2.4 mm diameter of welding electrode)	Amperage of 2nd and 3rd run of welding (3.25 mm diameter of welding electrode)	Angular distortion (10^{-2}) radians
80 A	100 A	0.549
100 A	125 A	1.707
125 A	150 A	0.601

Conclusions

The formation of angular distortions is greatly affected by a number of factors. Among these are the input current, geometry of the joint, the thickness of welded plates and the kind, thermal and mechanical properties of the welded plates and filler material. Generally speaking we can observe the following points.

- Angular distortions increase with increased current. This is true as long as that the melting of base plates does not reach the other side of the plate. If this happens some molten metal flows to the other side of the plates causing the distortion to decrease. A more sophisticated program is needed to account for the fluid flow of molten filler electrode which is not taken into account in the present FDM program.
- Angular distortions decrease with the increased number of opposite passes. The opposite side welding tends to eliminate the effect of each other. Shrinkages at opposite sides of the welding tend to eliminate each other effects. This is opposed by increasing welding expenses and efforts.
- Angular distortions decrease with the increased thickness of plates. This is due to the fact that each plate act by its own weight torque on the joint causing it to decrease.

- Square butt joints have fewer distortions than single-v joints. This is due to the fact that a contraction of the solidified filler molten material is equal both on the surface and inner part of the joint.
- FDM results are better than simple empirical results since it takes into account more thermal and mechanical effects on the formation of the joints.

Nomenclature

A – area, [m^2]
c – specific heat, [$Jkg^{-1}°C^{-1}$]
F_G – geometry coefficient
F_ε – emmisivity coefficient
H – plate thicknes, [mm]
h – heat transfer coefficient, [$Wm^{-2}°C^{-1}$]
I – current, [A]
Q – volumetric density of the power input, [Wm^{-3}]
q_c – heat transfer by convection, [Wm^{-2}]
q_r – heat transfer by radiation, [Wm^{-2}]
T – temperature, [°C]
T_S – softening material temperature, [°C]
T_w – surface temperature, [°C]
T_∞ – temperature of the surrounding fluid, [°C]
U – Voltage, [V]
v – welding speed, [mms^{-1}]

Greek letters

α – the thermal expansion coefficient
β – angular distorsion, [radians]
λ – thermal conductivity, [$Wm^{-1}K^{-1}$]
ρ – density, [kgm^{-3}]
σ – Stefan-Boltzman constant, [$Wm^{-2}k^{-4}$]
θ – groove angle, [radians]

Subscripts

∞ – surrounding fluid

Acronyms

FDM – finite difference method
FEM – finite element method

References

[1] Rosenthal, D., Schmerber, R., Thermal Study of Arc Welding, Experimental Verification of Theoretical Formulas, *Am. Weld. Journ, 17* (1938), 4, pp. 2s-8s
[2] Westby, O., Temperature Distribution in the Work-Piece by Welding, Ph. D. thesis, The Technical University of Norway, Trondheim, Norway, 1968
[3] Rappaz, M., Modelling of Microstructure Formation in Solidification Processes, *International Materials Review, 34* (1989), 3, pp. 93-123
[4] Igarashi, K., Method for Automatic Optimization of Finite Difference Grids in Simulator, United States Patent no. 5991526, 1999
[5] Okerblom, N. O., Technological and Structural Design of Welded Structures (in Russian), Mashinostroenie, Moscow, 1964
[6] Okerblom, N. O., The Calculations of Deformation of Welded Metal Structures (in Russian), Mashgiz, Moscow, 1955
[7] Shibib, K. S., Minshid, M. A., Tahir, M. M., Finite Element Analysis of Spot Laser of Steel Welding Temperature History, *Thermal Science, 13* (2009), 4, pp. 143-150
[8] Maiti, A., *et al*., Finite Element Simulation of Laser Spot Welding, *Science and Technology of Welding and Joining, 8* (2003), 5, pp. 377-384
[9] Jiang, W., Yahiaoui, K., Hall, F. R., Finite Element Predictions of Temperature Distributions in a Multipass Welded Piping Branch Junction, *J. Pressure Vessel Technol., 127* (2005), 1, pp. 7-13
[10] Frewin, M. R., Scott, D. A., Finite Element Model of Pulsed Laser Welding, *Welding Research Supplement* (1999), pp. 17s-22s
[11] Zhu, X. K., Chao, Y. J., Numerical Simulation of Transient Temperature and Residual Stresses in Friction stir Welding of 304L Stainless Steel, *Journal of Materials Processing Technology, 146* (2004), 2, pp. 263-272
[12] Abida, M., Siddique, M., Numerical Simulation to Study the Effect of Tack Welds and Root Gap on Welding Deformations and Residual Stresses of a Pipe-Flange Joint, *International Journal of Pressure Vessels and Piping, 82* (2005), 11, pp. 860-871

[13] Yaghia, A., *et al*., Residual Stress Simulation in Thin and Thick-Walled Stainless Steel Pipe Welds Including Pipe Diameter Effects, *International Journal of Pressure Vessels and Piping, 83* (2006), 11-12, pp. 864-874
[14] Mackerle, J., Finite Element Analysis and Simulation of Welding: a Bibliography (1976-1996), *Modelling Simul. Mater. Sci. Eng., 4* (1996), 5, pp. 501-533
[15] Koseki ,T., *et al*., Numerical Simulation of Equiaxed Grain Formation in Weld Solidification, *Science and Technology of Advanced, 4* (2003), 2, pp. 183-195
[16] Mezrhab, A., Bouzidi, M., Lallemand, P., Hybrid Lattice-Boltzmann Finite-Difference Simulation of Convective Flows, *Computers & Fluids, 33* (2004), 4, pp. 623-641
[17] Costa, M., Buddhi, D., Olivia, A., Numerical Simulation of a Latent Heat Thermal Energy Storage System with Enhanced Heat Conduction, *Energy Conversion and Management, 39* (1998), 3-4, pp. 319-330
[18] Andrés, E., *et al*., A Hybrid Spectral/Finite-Difference Large-Eddy Simulator of Turbulent Processes in the Upper Ocean, *Ocean Modelling, 30* (2009), 2-3, pp. 115-142
[19] Tamura, A., Tsutahara, M., Kataoka, T., Numerical Simulation of Two-Dimensional Blade-Vortex Interactions Using Finite Difference Lattice Boltzmann Method, *AIAA Journal, 46* (2008), 9, pp. 2235-2247
[20] Grzesik, W., Bartoszuk, M., Prediction of Temperature Distribution in the Cutting Zone using Finite Difference Approach, *International Journal of Machining and Machinability of Materials, 6* (2009), 1-2, pp. 43-53
[21] Bakier, A. Y., Mansour, M. A., Combined of Magnetic Field and Thermophoresis Particle Deposition in Free Convection Boundary Layer from a Vertical Flat Plate Embedded in a Porous Medium, *Thermal Science, 11* (2007), 1, pp. 65-74
[22] Mohammed, H. A., Salman, Y. K., Numerical Study of Combined Convection Heat Transfer for Thermally Developing upward Flow in a Vertical Cylinder, *Thermal Science, 12* (2008), 2, pp. 89-102
[23] Callister, W. D., Materials Science and Engineering: An Introduction, John Wiley & Sons, Inc., New York, USA, 2000
[24] Hughes, W. F., Gaylord, E. W., Schaum's Outline Series in Basic Equations of Engineering Science, McGraw-Hill, USA, 1964

Paper submitted: February 6, 2010
Paper revised: March 17, 2010
Paper accepted: May 22, 2010